

Supporting Information

Nanoarchitectonics of Bacterial Cellulose with Nickel-Phosphorous Alloy as a Binder-Free Electrode for Efficient Hydrogen Evolution Reaction in Neutral Solution

Wenhai Wang,^a Siavash Khabazian,^b Marina Casas Papiol,^a Soledad Roig-Sanchez,^a Anna Laromaine,^a Anna Roig,^a Dino Tonti^{a*}

^a *Institut de Ciència de Materials de Barcelona (ICMAB-CSIC), Campus UAB, 08193 Bellaterra, Spain*

^b *Nanomaterials Group, Department of Materials Science and Engineering, Tarbiat Modares University, Tehran, Iran*

*Corresponding author. E-mail address: dino.t@csic.es (D. Tonti).

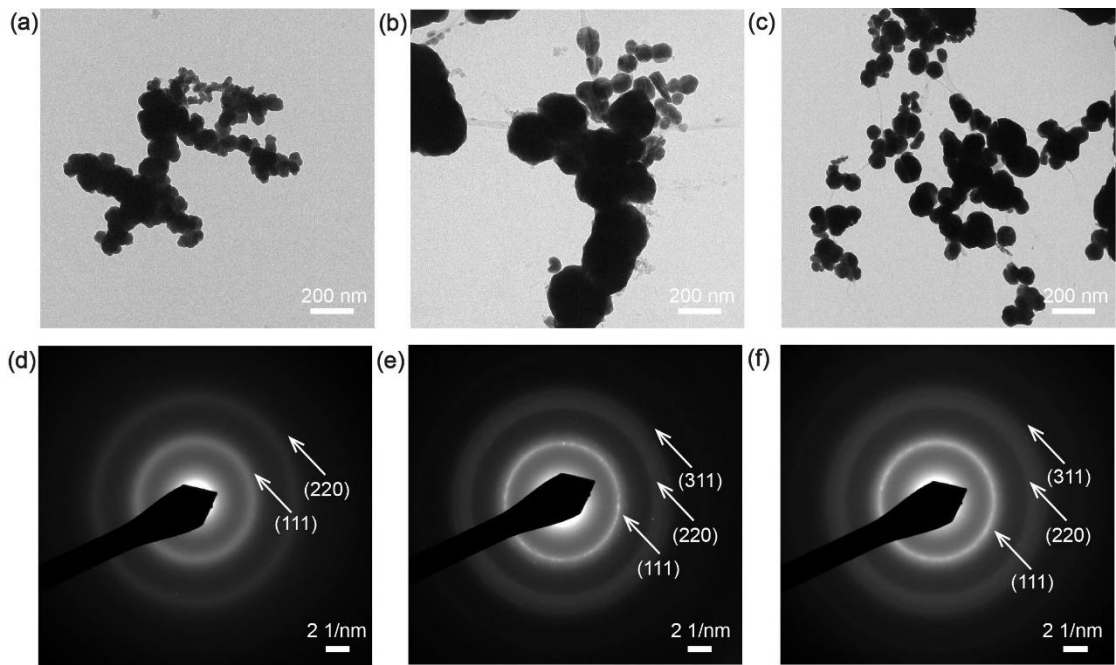


Figure S1. TEM images of (a) Ni-B-1/BC, (b) Ni-B-2/BC and (c) Ni-P/BC; SAED patterns of (d) Ni-B-1/BC, (e) Ni-B-2/BC and (f) Ni-P/BC.

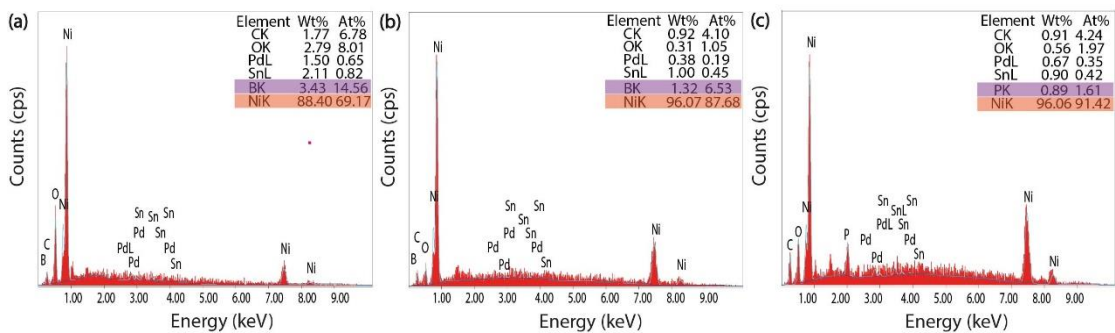


Figure S2. EDX spectra of (a) Ni-B-1/BC, (b) Ni-B-2/BC and (c) Ni-P/BC

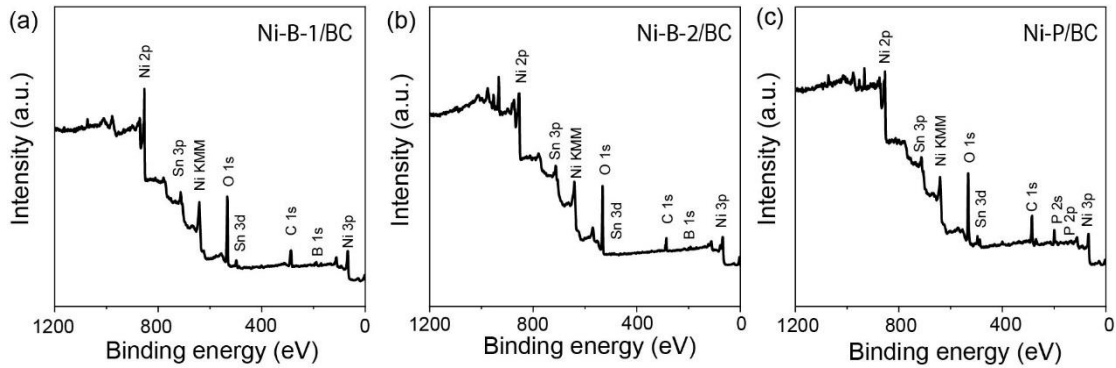


Figure S3. XPS survey for elements of (a) Ni-B-1/BC, (b) Ni-B-2/BC and (c) Ni-P/BC.

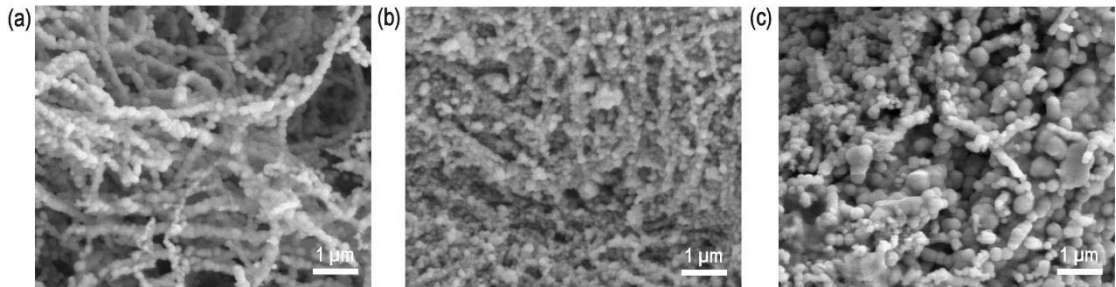


Figure S4. SEM images for different deposition times for Ni-P grown on BC: (a) 10 m, (b) 20 m and (c) 30 m.

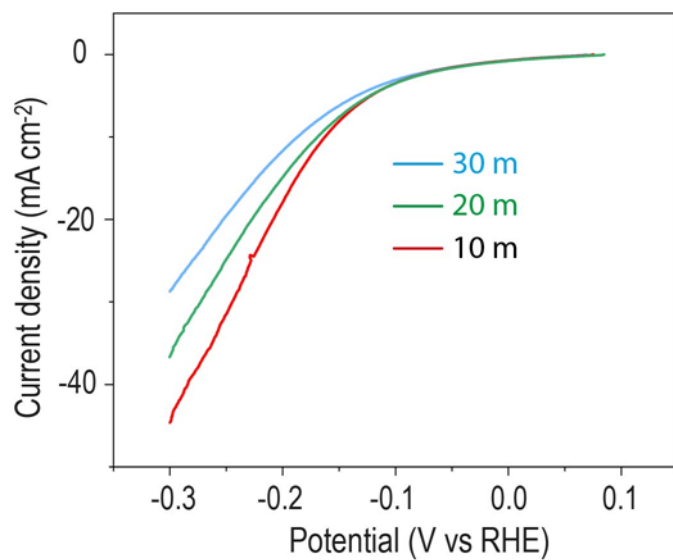


Figure S5. HER polarization curves of different deposition time for Ni-P grown on BC.

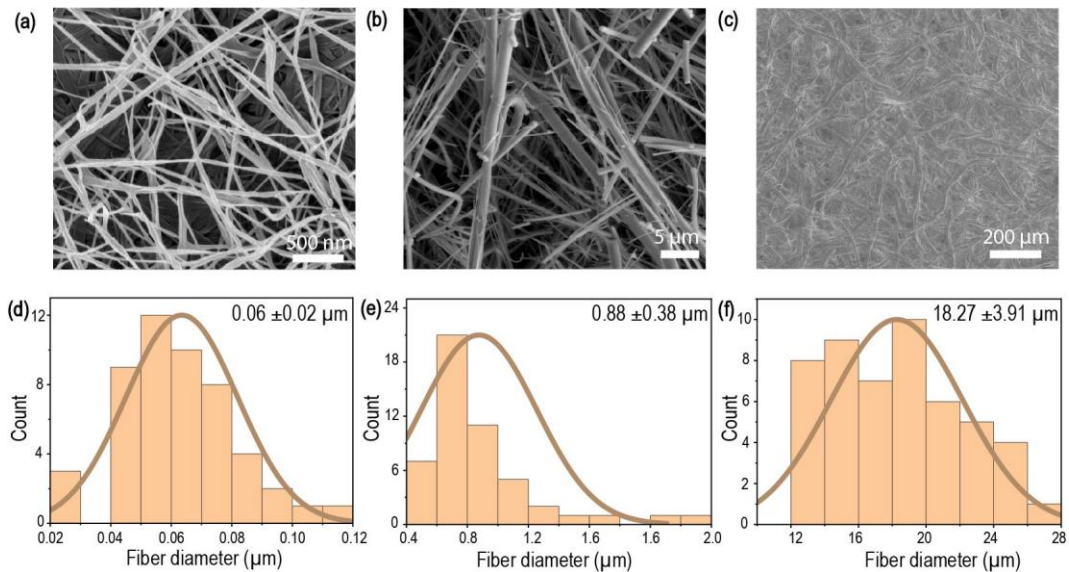


Figure S6. SEM images of (a) BC, (b) GFP and (c) FP. Fiber diameter histograms of (d) BC, (e) GFP and (f) FP obtained by manual measures on the images using the ImageJ software.

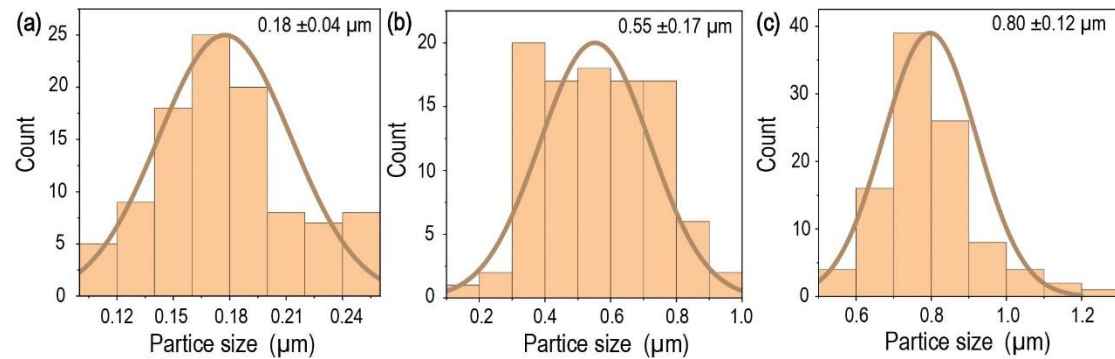


Figure S7. Ni-P nanoparticle size histograms of (a) Ni-P/BC, (b) Ni-P/GFP and (c) Ni-P/FP obtained by manual measures on the images using the ImageJ software.

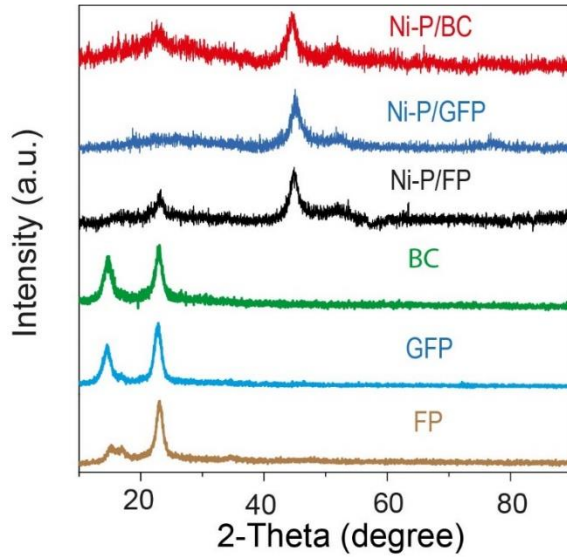


Figure S8. XRD patterns of Ni-P/BC, Ni-GFP, Ni-P/FP, BC, GFP and FP.

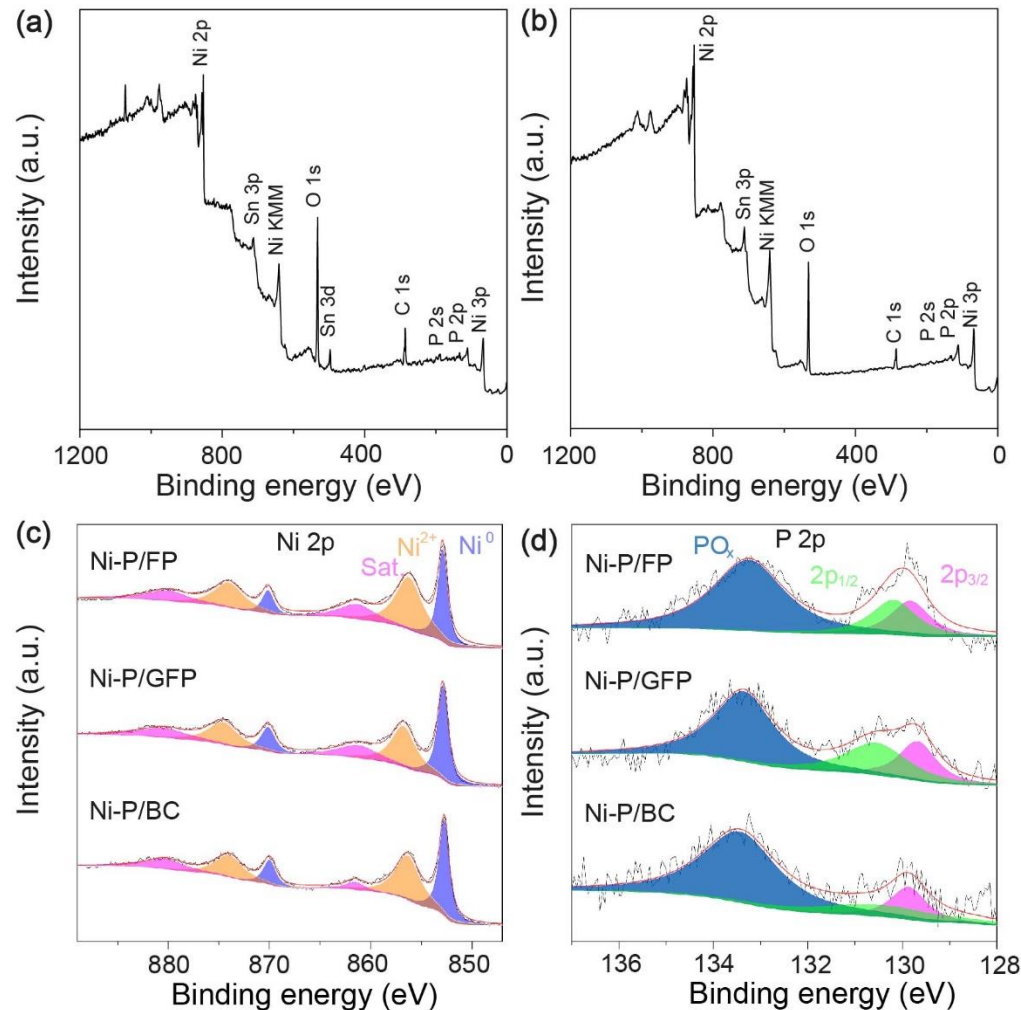


Figure S9. XPS survey for elements of (a) Ni-P/FP, (b) Ni-P/GFP. (c) XPS spectra of Ni 2p. (d) XPS spectra of P 2p.

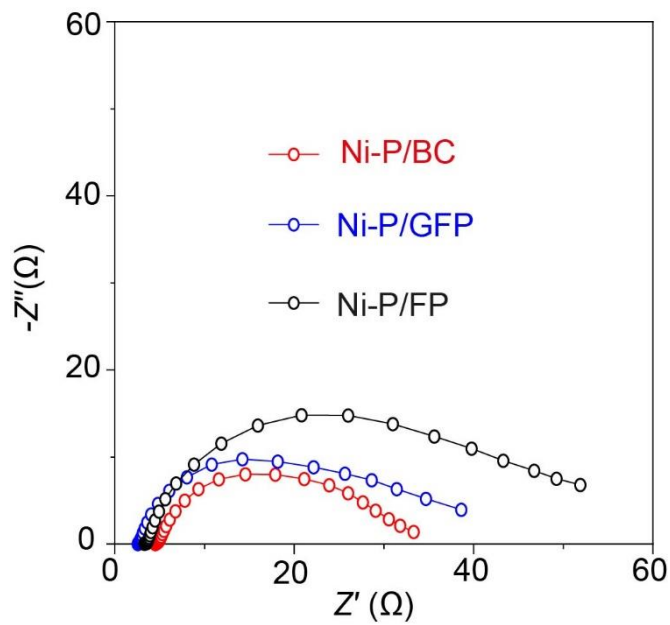


Figure S10. Electrochemical impedance spectra of Ni-P/BC, Ni-GFP and Ni-P/FP at 150 mV overpotential.

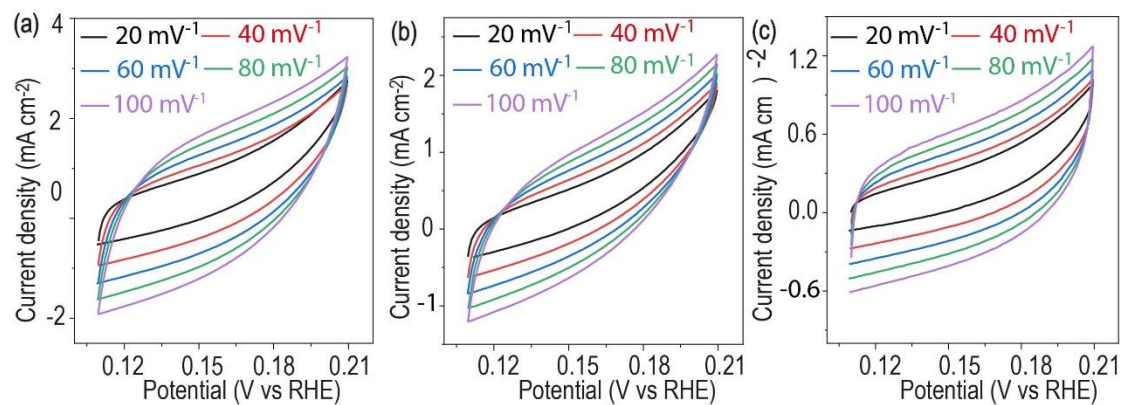


Figure S11. CV curves of (a) Ni-P/BC, (b) Ni-P/GFP and (c) Ni-P/FP at different scan rates.

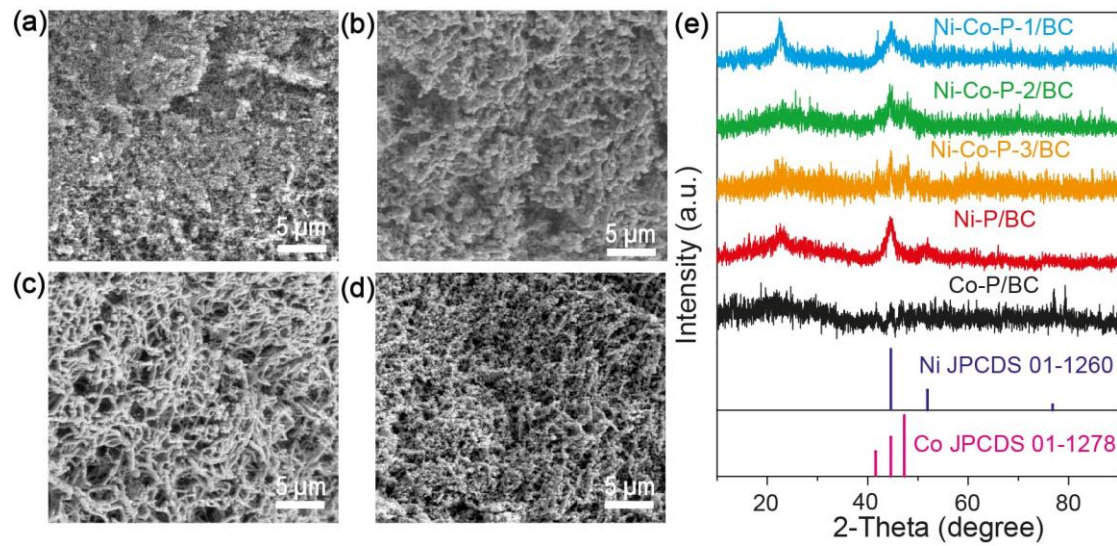


Figure S12. SEM images of (a) Co-P/BC, (b) Ni-Co-P-3/BC, (c) Ni-Co-P-2/BC and Ni-Co-P-3/BC. (e) XRD patterns of samples.

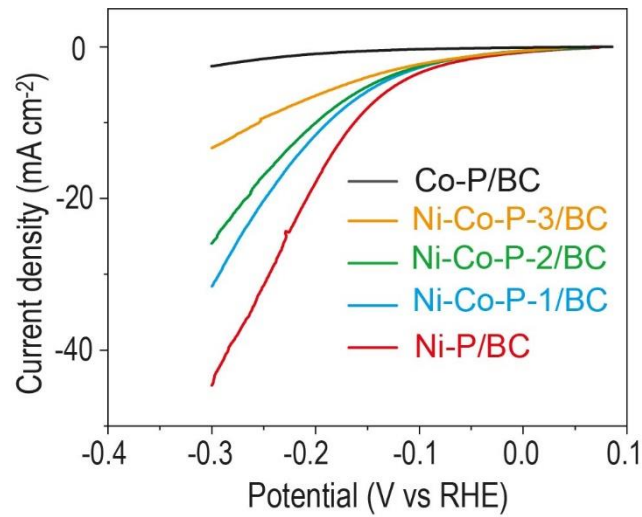


Figure S13. HER polarization curves of electrodes.

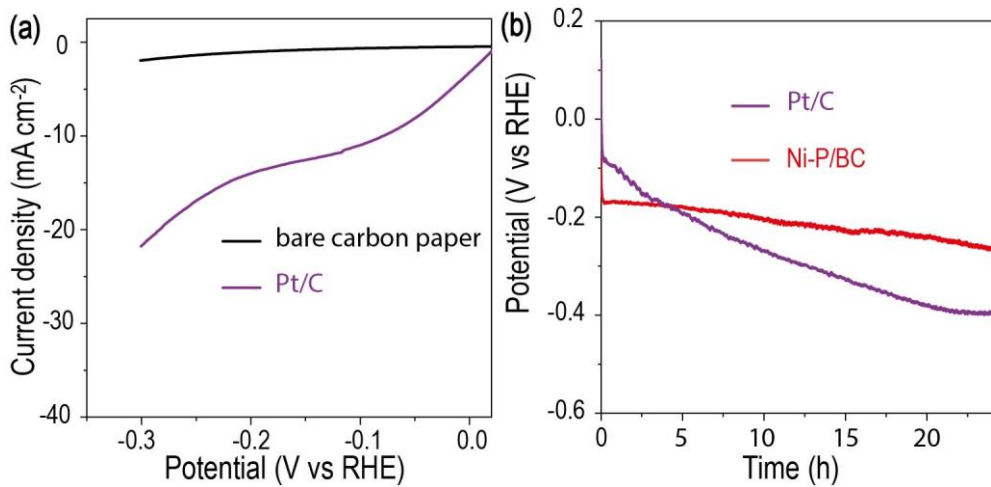


Figure S14. (a) HER polarization curves of bare carbon paper and Pt/C. (b) Chronopotentiometry curves of Ni-P/BC and Pt/C at 10 mA cm^{-2} .

Table S1 XPS binding energies of Ni 2p for Ni-B-1/BC, Ni-B-2/BC and Ni-P/BC.

Sample	2p _{3/2}			2p _{1/2}		
	Ni ⁰ (eV)	Ni ²⁺ (eV)	Satellite (eV)	Ni ⁰ (eV)	Ni ²⁺ (eV)	Satellite (eV)
Ni-B-1/BC	853.1	856.6	859.6	870.4	874.6	879.4
Ni-B-2/BC	852.9	856.1	861.3	870.2	874.0	879.8
Ni-P/BC	852.8	856.3	861.5	870.0	874.0	880.3

Table S2 XPS binding energies of B 1s for Ni-B-1/BC and Ni-B-2/BC.

Sample	BO _x (eV)	B ⁰ (eV)
Ni-B-1/BC	192.2	188.5
Ni-B-2/BC	191.7	188.4

Table S3 Series resistance of Ni-B-1/BC, Ni-B-2/BC and Ni-P/BC

Sample	Series resistance (Ω)
Ni-B-1/BC	23.1
Ni-B-2/BC	4.5
Ni-P/BC	4.7

Table S4 XPS binding energies of Ni 2p for Ni-P/BC, Ni-P/GFP and Ni-P/FP.

Sample	2p _{3/2}			2p _{1/2}		
	Ni ⁰ (eV)	Ni ²⁺ (eV)	Satellite (eV)	Ni ⁰ (eV)	Ni ²⁺ (eV)	Satellite (eV)
Ni-P/BC	852.8	856.3	861.5	870.0	874.0	880.3
Ni-P/GFP	852.9	856.8	861.2	870.1	874.6	880.5
Ni-P/FP	852.9	856.2	861.3	870.1	874.0	880.1

Table S5 XPS binding energies of P 2p for Ni-P/BC, Ni-P/GFP and Ni-P/FP.

Sample	P ⁰		PO _x (eV)
	2p _{1/2} (eV)	2p _{3/2} (eV)	
Ni-P/BC	130.4	129.9	133.4
Ni-P/GFP	130.5	129.7	133.4
Ni-P/FP	130.2	129.8	133.3

Table S6 Comparison of the HER activity of prepared electrodes in 1 M PBS (pH=7) at 10 mA cm⁻².

Sample	Overpotential (mV)
Ni-B-1/BC	>>300
Ni-B-2/BC	269
Ni-P/BC	161
Ni-P/GFP	202
Ni-P/FP	252

Note: Ni-B-1/BC demonstrates poor HER performance than others and the maximum current density of Ni-B-1/BC is 2.4 mA cm⁻², which is much lower than 10 mA cm⁻².

Table S7 Comparison of the HER activity with other electrodes in 1 M PBS (pH=7).

Electrode	Substrate	Overpotential (mV at 10 mA cm ⁻²)	Preparation method	Reference
Ni-P/BC	bacterial cellulose	161	electroless deposition	This work
Ru SAs-Ni ₂ P	glassy carbon	260	calcination	[1]
NiP _x	carbon cloth	230	electrochemical deposition	[2]
Ni ₂ P	carbon paper	196	electrochemical deposition	[3]
NiP ₂ -CC nanohybrids	carbon cloth	160	calcination	[4]
MoP NA/CC	carbon cloth	187	calcination	[5]
CoS _x -(0.2-0.02)-12	FTO	168	electrochemical deposition	[6]
CoMoS ₄ NS/CC	carbon cloth	183	hydrothermal reaction	[7]
Ni ₃ S ₂ /NF	Ni foam	170	hydrothermal reaction	[8]
MoP700	glassy carbon	196	calcination	[9]
Karst NF	Ni foam	110	electrochemical deposition	[10]

References

- [1] K. Wu, K. Sun, S. Liu, W.-C. Cheong, Z. Chen, C. Zhang, Y. Pan, Y. Cheng, Z. Zhuang, X. Wei, Y. Wang, L. Zheng, Q. Zhang, D. Wang, Q. Peng, C. Chen, Y. Li, *Nano Energy*, 80 (2021) 105467.
- [2] M. Chen, J. Qi, W. Zhang, R. Cao, *Chem. Commun.*, 53 (2017) 5507-5510.
- [3] R. Wu, B. Xiao, Q. Gao, Y.R. Zheng, X.S. Zheng, J.F. Zhu, M.R. Gao, S.H. Yu, *Angew. Chem. Int. Edit.*, 57 (2018) 15445-15449.
- [4] Y. Ding, B.-Q. Miao, Y.-C. Jiang, H.-C. Yao, X.-F. Li, Y. Chen, *J. Mater. Chem. A.*, 7 (2019) 13770-13776.
- [5] Z. Pu, S. Wei, Z. Chen, S. Mu, *Appl. Catal., B*, 196 (2016) 193-198.
- [6] W. He, R. Ifraimov, A. Raslin, I. Hod, *Adv. Funct. Mater.*, 28 (2018) 1707244.
- [7] X. Ren, D. Wu, R. Ge, X. Sun, H. Ma, T. Yan, Y. Zhang, B. Du, Q. Wei, L. Chen, *Nano Research*, 11 (2018) 2024-2033.
- [8] L.L. Feng, G. Yu, Y. Wu, G.D. Li, H. Li, Y. Sun, T. Asefa, W. Chen, X. Zou, *J. Am. Chem. Soc.*, 137 (2015) 14023-14026.
- [9] X. Xie, M. Song, L. Wang, M.H. Engelhard, L. Luo, A. Miller, Y. Zhang, L. Du, H. Pan, Z. Nie, Y. Chu, L. Estevez, Z. Wei, H. Liu, C. Wang, D. Li, Y. Shao, *ACS Catal.*, 9 (2019) 8712-8718.
- [10] X. Gao, Y. Chen, T. Sun, J. Huang, W. Zhang, Q. Wang, R. Cao, *Energy Environ. Sci.*, 13 (2020) 174-182.